

# Condensed Matter and Interphases (Kondensirovannye sredy i mezhfaznye granitsy)

## Original articles

DOI: <https://doi.org/10.17308/kcmf.2020.22/2835>

Received 28 January 2020

Accepted 15 May 2020

Published online 25 June 2020

ISSN 1606-867X

eISSN 2687-0711

## The study of the quasi-triple system $\text{FeS}-\text{Ga}_2\text{S}_3-\text{Ag}_2\text{S}$ by a $\text{FeGa}_2\text{S}_4-\text{AgGaS}_2$ section

©2020 Sh. H. Mammadov

*Institute of Catalysis and Inorganic Chemistry named after Academician M. F. Nagiyev  
of the National Academy of Sciences of Azerbaijan,  
113 G. Javid pr., Baku Az1143, Azerbaijan*

### Abstract

The interest in the study of systems containing sulphides with the formula  $A^I B^III C^VI_2$  is generated in particular by emerging opportunities for their practical use in the production of non-linear optical devices, detectors, solar cells, photodiodes, luminophors, etc. Therefore, taking into account the search for new promising materials based on silver and iron thiogallates, the goal of this work is to study the quasi-binary section  $\text{FeGa}_2\text{S}_4-\text{AgGaS}_2$  of the quaternary system  $\text{Fe}-\text{Ag}-\text{Ga}-\text{S}$ .

The alloys of the  $\text{AgGaS}_2-\text{FeGa}_2\text{S}_4$  system were synthesised from high-purity base metals: iron – 99.995 %, gallium – 99.999 %, silver – 99.99 %, and sulphur – 99.99 %. The alloys were studied using differential thermal analysis, X-ray phase analysis, and microstructural analysis as well as microhardness measurement and density determination.

Using the methods of physicochemical analysis, a  $T-x$  phase diagram of the  $\text{AgGaS}_2-\text{FeGa}_2\text{S}_4$  section, which is the internal section of the quasi-triple  $\text{FeS}-\text{Ga}_2\text{S}_3-\text{Ag}_2\text{S}$  system, was studied and constructed for the first time. It was established that this system is of the simple eutectic type. The composition of the eutectic point is 56 mol%  $\text{FeGa}_2\text{S}_4$  and  $T = 1100$  K. The solid solution ranges were determined on the basis of the source components. Based on  $\text{FeGa}_2\text{S}_4$  and  $\text{AgGaS}_2$  at the eutectic temperature the solubility stretches to 10 and 16 mol% respectively. With decreasing temperature, the solid solutions narrow and, at room temperature, comprise 4 mol%  $\text{AgGaS}_2$  based on iron thiogallate ( $\text{FeGa}_2\text{S}_4$ ) and 11 mol%  $\text{FeGa}_2\text{S}_4$  based on silver thiogallate ( $\text{AgGaS}_2$ ).

**Keywords:** phase diagram, solid solution,  $\text{FeGa}_2\text{S}_4$ ,  $\text{AgGaS}_2$ , quasi-triple system, eutectic, X-ray analysis,  $\text{FeS}-\text{Ga}_2\text{S}_3-\text{Ag}_2\text{S}$ .

**For citation:** Mammadov Sh. H. The study of the quasi-triple system  $\text{FeS}-\text{Ga}_2\text{S}_3-\text{Ag}_2\text{S}$  by a  $\text{FeGa}_2\text{S}_4-\text{AgGaS}_2$  section. *Kondensirovannye sredy i mezhfaznye granitsy = Condensed Matter and Interphases*. 2020;22(2): 232–237. DOI: <https://doi.org/10.17308/kcmf.2020.22/2835>

### 1. Introduction

The interest in the study of systems containing sulphides with the formula  $A^I B^III C^VI_2$  is generated in particular by emerging opportunities for their practical use in the production of non-linear optical devices, detectors, solar cells, photodiodes, luminophors, etc. [1–17].

The reported data shows that multicomponent sulphide compounds, especially those containing magnetic ( $\text{FeGa}_2\text{S}_4$ ,  $\text{Fe}_2\text{Ga}_2\text{S}_5$ ,  $\text{FeIn}_2\text{S}_4$ , etc.) ions, are functional materials and are used in the production of magneto-optical devices, photodetectors, lasers, light modulators, etc. [18–25].

The source components comprising the quaternary system  $\text{Ag}-\text{Fe}-\text{Ga}-\text{S}$  were thoroughly studied in [26–42]. Compositions  $\text{AgGaS}_2$ ,  $\text{Ag}_9\text{GaS}_6$ , and  $\text{Ag}_2\text{Ga}_{20}\text{S}_{31}$  were established during the study of the  $\text{Ag}_2\text{S}-\text{Ga}_2\text{S}_3$  binary system [26, 30, 31].  $\text{Ag}_2\text{Ga}_{20}\text{S}_{31}$  is formed from them by a peritectic reaction at 1268 K while  $\text{AgGaS}_2$  and  $\text{Ag}_9\text{GaS}_6$  melt congruently at 1270 and 1063 K respectively.  $\text{AgGaS}_2$  crystallises within the chalcopyrite-type structure ( $a = 5.7544$ ,  $c = 10.299$  Å space group I42d) [27] and is a  $p$ -type semiconductor with a band gap of  $\Delta E = 2.75$  eV [32].

The phase diagram of the section  $\text{Ga}_2\text{S}_3-\text{FeS}$  was studied in [33–42]. The authors established

✉ Sharafat Hajiaga Mammadov, e-mail: [azxim@mail.ru](mailto:azxim@mail.ru)



The content is available under Creative Commons Attribution 4.0 License.

that triple compounds  $\text{FeGa}_2\text{S}_4$  and  $\text{Fe}_2\text{Ga}_2\text{S}_5$  are formed in the system  $\text{Ga}_2\text{S}_3\text{-FeS}$  [38, 42].

The microhardness of the  $\text{FeGa}_2\text{S}_4$  and  $\text{Fe}_2\text{Ga}_2\text{S}_5$  compounds are  $4000 \pm 5$  and  $3500 \pm 5$  MPa respectively [42].

The  $\text{FeGa}_2\text{S}_4$  compound melts congruently at 1418 K [38], although, according to [39],  $\text{FeGa}_2\text{S}_4$  is formed by a peritectic reaction at 1343 K and undergoes polymorphous transformation at 1283 K.  $\text{FeGa}_2\text{S}_4$  crystallises in a rhombic crystal system of the  $\text{ZnAl}_2\text{S}_4$  type with the following parameters:  $a = 1.289$  nm,  $b = 0.751$ ,  $c = 0.609$  nm [40]. According to [41], this compound has two crystalline modifications: low-temperature trigonal P3ml:  $a = 0.3654$  nm,  $c = 1.2056$  nm; and high-temperature rhombic:  $a = 1.289$ ,  $b = 0.751$ ,  $c = 0.609$  nm.

The goal of this work is to study the quasi-binary section  $\text{FeGa}_2\text{S}_4\text{-AgGaS}_2$  of the quaternary system  $\text{Fe-Ag-Ga-S}$ .

## 2. Experimental

Synthesis of the alloys of the  $\text{AgGaS}_2\text{-FeGa}_2\text{S}_4$  system were conducted from base metals. The base metals ( $\text{AgGaS}_2$  and  $\text{FeGa}_2\text{S}_4$ ) were synthesised using high-purity: iron – 99.995 %, gallium – 99.999 %, silver – 99.99 %, and sulphur – 99.99 %. Stoichiometric mixtures of the elements were placed in vacuum quartz ampoules (17 cm long and 1.5 cm in diameter) with residual pressure  $\sim 0.133$  Pa [43]. Then the ampoule was placed in a two-zone furnace. The furnace was slowly heated from room temperature to the fusion temperature of the compound  $\text{FeGa}_2\text{S}_4$ . Sulphur becomes condensed in the cold region and returns to the interaction zone. The alloys in a liquid state were stirred at regular intervals. The outer part of the ampoule was cooled with water. After 1.5–2 hours in the cold region, the mass of the sulphur decreased. After that, the whole ampoule was placed in the furnace and held at a temperature of 1450 K for 2.5 hours. The process of synthesis lasted for at least 4 hours. Then the obtained samples were homogenised at a temperature of 800 K for 150 h. The alloys were studied using differential thermal analysis (DTA), X-ray phase analysis (XRD), and microstructural analysis (MSA) as well as microhardness measurement and density determination. XRD was performed on a D2 PHASER using Ni-filtered  $\text{CuK}_\alpha$  radiation.

DTA of the alloys of the system was conducted on an HTP-73 device with a heating rate of 10 degrees per minute. Calibrating chromel-alumel thermocouples were used with  $\text{Al}_2\text{O}_3$  as a reference standard. An etchant of the composition  $\text{NH}_4\text{NO}_3$  (3–8 wt%) +  $\text{K}_2\text{Cr}_2\text{O}_7$  (0.02–0.5 wt%) + conc.  $\text{H}_2\text{SO}_4$  was used during the study of the microstructure of the alloys with the etching time of 20 sec. The microhardness of the alloys was measured on a microhardness tester PMT-3 at the loads 0.01 and 0.02 N. MSA of the system alloys was performed on a MIM-8 metallographic microscope on preliminarily etched sections polished with the paste.

## 3. Results and discussion

Based on the results of physicochemical analysis (DTA, XRD, MSA, and density determination), a phase diagram of the system  $\text{AgGaS}_2\text{-FeGa}_2\text{S}_4$  was developed. The DTA results showed that all thermograms of the system alloys (90–10 mol%  $\text{AgGaS}_2$ ) have three endoeffects each, except for the alloy containing 56 mol%  $\text{FeGa}_2\text{S}_4$  while the alloys containing 90 and 10 mol%  $\text{AgGaS}_2$  demonstrate two and four endoeffects each respectively (Table 1). The effects at 905 K correspond to the phase transition  $\alpha\text{-FeGa}_2\text{S}_4 \leftrightarrow \beta\text{-FeGa}_2\text{S}_4$ .

As Fig. 1 shows, the phase diagram of the system  $\text{AgGaS}_2\text{-FeGa}_2\text{S}_4$  belongs to the eutectic type with limited component solubility in solid state. The solubility at 300 K based on  $\text{AgGaS}_2$  is

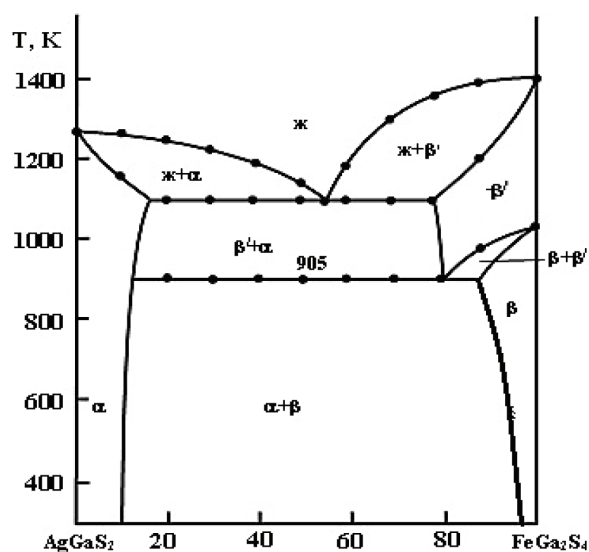


Fig. 1. Phase diagram of the  $\text{AgGaS}_2\text{-FeGa}_2\text{S}_4$  system

**Table 1.** Composition, results of the DTA of alloys of the AgGaS<sub>2</sub>–FeGa<sub>2</sub>S<sub>4</sub> system

Composition mol% FeGa <sub>2</sub> S <sub>4</sub>	Thermal effects, K
100	1420
90	905, 980, 1235, 1405
80	905, 1100, 1375
70	905, 1100, 1310
60	905, 1100, 1175
56	1100 (eutectic)
50	905, 1100, 1145
40	905, 1100, 1195
30	905, 1100, 1230
20	905, 1100, 1250
10	1175, 1260
0.0	1270

11 mol% FeGa<sub>2</sub>S<sub>4</sub> and 4 mol% AgGaS<sub>2</sub> based on FeGa<sub>2</sub>S<sub>4</sub>. The solubility at the eutectic temperature stretches to 16 and 10 mol% respectively. The eutectic has a composition of 56 mol% FeGa<sub>2</sub>S<sub>4</sub> and crystallises at 1100 K.

The liquidus of the system AgGaS<sub>2</sub>–FeGa<sub>2</sub>S<sub>4</sub> consists of the primary crystallisation branches  $\alpha$  and  $\beta$  solid solutions crossing at 56 mol% FeGa<sub>2</sub>S<sub>4</sub> and  $T = 1100$  K. The temperature of the phase transition  $\beta(\text{FeGa}_2\text{S}_4) \leftrightarrow \beta'(\text{FeGa}_2\text{S}_4)$  is reduced to 905 K under the influence of the second component. MSA of the annealed alloys showed that the alloys of the system AgGaS<sub>2</sub>–FeGa<sub>2</sub>S<sub>4</sub> are single-phase except for the alloys containing 11–96 mol% FeGa<sub>2</sub>S<sub>4</sub>.

Below solidus,  $\alpha$  and  $\beta$  solid solutions co-crystallise. The solubility regions based on source components are narrow: 11 mol% FeGa<sub>2</sub>S<sub>4</sub> based on AgGaS<sub>2</sub> and 4 mol% AgGaS<sub>2</sub> based on the second component. Solubility limits were determined using the XRD and MSA of the alloys annealed and quenched at the temperature 700 K.

To determine the limits of the regions of solid solutions of the source components (AgGaS<sub>2</sub> and FeGa<sub>2</sub>S<sub>4</sub>), 98, 96, 95, 93, 91, 90, 89, 88 mol% were additionally synthesised from both sides. These alloys were annealed at 650 and 800 K with the annealing duration of 1 month (Table 2).

After the annealing, a microstructural analysis of the alloys was conducted that showed that there are limited solubility regions near AgGaS<sub>2</sub> and FeGa<sub>2</sub>S<sub>4</sub>. Solid solutions based on AgGaS<sub>2</sub> belong to the Ag<sub>2</sub>GeS<sub>3</sub> structural type and

**Table 2.** Annealing of the alloys of the AgGaS<sub>2</sub>–FeGa<sub>2</sub>S<sub>4</sub> system at temperatures of 650 and 800 K

Composition mol%		650 K phase count	800 K, phase count
AgGaS <sub>2</sub>	FeGa <sub>2</sub> S <sub>4</sub>		
0.0	100	$\alpha$	$\alpha$
2.0	98	$\alpha$	$\alpha$
4.0	96	$\alpha+\beta$	$\alpha$
5.0	95	$\alpha+\beta$	$\alpha+\beta$
7.0	93	$\alpha+\beta$	$\alpha+\beta$
9.0	91	$\alpha+\beta$	$\alpha+\beta$
10	90	$\alpha+\beta$	$\alpha+\beta$
11	89	$\alpha+\beta$	$\alpha+\beta$
12	88	$\alpha+\beta$	$\alpha+\beta$
100	0.0	$\beta$	$\beta$
98	2.0	$\beta$	$\beta$
96	4.0	$\beta$	$\beta$
95	5.0	$\beta$	$\beta$
93	7.0	$\beta$	$\beta$
91	9.0	$\beta$	$\beta$
90	10	$\alpha+\beta$	$\beta$
89	11	$\alpha+\beta$	$\beta$
88	12	$\alpha+\beta$	$\alpha+\beta$

crystallise in the monoclinic syngony. Within the solubility limits, the parameters of the crystal lattice increase:  $a = 0.627 \div 0.748$ ,  $b = 0.580 \div 0.664$ ,  $c = 1.318 \div 1.386$  nm,  $\beta = 93.27 \div 93^\circ 61$ .

The results of the X-ray phase analysis are in good agreement with the data of the microstructural analysis and confirm the formation of solid solutions based on the source components in the system AgGaS<sub>2</sub>–FeGa<sub>2</sub>S<sub>4</sub>.

The data of the X-ray powder patterns of the alloys of the system AgGaS<sub>2</sub>–FeGa<sub>2</sub>S<sub>4</sub> showed that the samples of the compositions 0–11 and 95–100 mol% FeGa<sub>2</sub>S<sub>4</sub> are single-phase. Their diffraction lines are identical to the diffraction patterns of the source components (silver thiogallate and iron thiogallate). The diffraction pattern of the alloys containing 11–96 mol% FeGa<sub>2</sub>S<sub>4</sub> is two-phase (Fig. 2).

#### 4. Conclusions

1. Using the methods of physicochemical analysis (XRD, DTA, MSA), a phase diagram of the system AgGaS<sub>2</sub>–FeGa<sub>2</sub>S<sub>4</sub> was studied and constructed for the first time. It was established that the system is a quasi-binary cross-section of the FeS–Ga<sub>2</sub>S<sub>3</sub>–Ag<sub>2</sub>S quasi-triple system and belongs to the simple eutectic type.

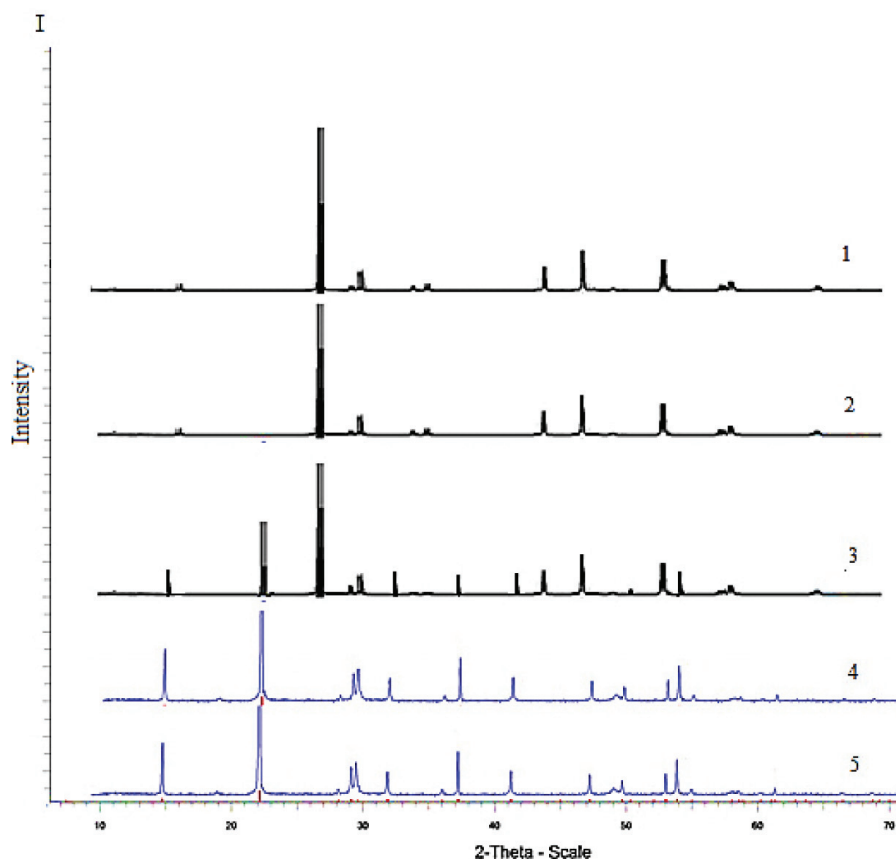


**Fig. 2.** Diffraction pattern of the alloys of the  $\text{AgGaS}_2\text{-FeGa}_2\text{S}_4$  system: 1 –  $\text{AgGaS}_2$ ; 2 – 11 mol%  $\text{FeGa}_2\text{S}_4$ ; 3 – 40 mol%  $\text{FeGa}_2\text{S}_4$ ; 4 – 96 mol%  $\text{FeGa}_2\text{S}_4$ ; 5 –  $\text{FeGa}_2\text{S}_4$

2. The formation of solid solutions based on their source components was found in the  $\text{AgGaS}_2\text{-FeGa}_2\text{S}_4$  system. The solubility based on iron thiogallate at room temperature is 4 mol%  $\text{AgGaS}_2$  and the solubility based on silver thiogallate is 11 mol%  $\text{FeGa}_2\text{S}_4$ .

### Conflict of interests

The author declares that they have no known competing financial interests or personal relationships that could have appeared to influence the work reported in this paper.

### References

1. Zhao B., Zhu S., Li Z., Yu F., Zhu X., Gao D. Growth of  $\text{AgGaS}_2$  single crystal by descending crucible with rotation method and observation of properties. *Chinese Sci. Bull.* 2001;46(23): 2009–2013. DOI:
2. Goryunova N. A. Slozhnyealmazopodobnye poluprovodniki [Complex diamond-like semiconductors]. Moscow: Sov. radio. Publ.; 1968. 215 c. (In Russ.)
3. Abrikosov N. Kh., Shelimova L. E. Poluprovodnikovye materialy na osnove soedinenii

$\text{A}^{\text{IV}}\text{B}^{\text{VI}}$  [Semiconductor materials based on compounds  $\text{A}^{\text{IV}}\text{B}^{\text{VI}}$ ]. Moscow: Nauka Publ.; 1975. 195 p. (In Russ.)

4. Kushwaha A. K., Khenata R., Bouhemadou A., Bin-Omran S., Haddadi K. Lattice dynamical properties and elastic constants of the ternary chalcopyrite compounds  $\text{CuAlS}_2$ ,  $\text{CuGaS}_2$ ,  $\text{CuInS}_2$ , and  $\text{AgGaS}_2$ . *Journal of Electronic Materials.* 2017;46(7): 4109–4118. DOI: <https://doi.org/10.1007/s11664-017-5290-6>

5. Uematsu T., Doi T., Torimoto T., Kuwabata S. Preparation of luminescent  $\text{AgInS}_2\text{-AgGaS}_2$  solid solution nanoparticles and their optical properties. *The Journal of Physical Chemistry Letters.* 2010;1(22): 3283–3287. DOI: <https://doi.org/10.1021/jz101295w>

6. Karaagac H., Parlak M. The investigation of structural, electrical, and optical properties of thermal evaporated  $\text{AgGaS}_2$  thin films. *J. Thin Solid Films.* 2011;519(7): 2055–2061. DOI: <https://doi.org/10.1016/j.tsf.2010.10.027>

7. Karunakaran N., Ramasamy P. Synthesis, growth and physical properties of silver gallium sulfide single crystals. *Materials Science in Semiconductor Processing.* 2016;41: 54–58. DOI: <https://doi.org/10.1016/j.mssp.2015.08.012>

8. Zhou H., Xiong L., Chen L., Wu L. Dislocations that decrease size mismatch within the lattice leading to ultrawide band gap, large second-order susceptibility,

- and high nonlinear optical performance of AgGaS<sub>2</sub>. *Angewandte Chemie International Edition*. 2019;58(29): 9979–9983. DOI: <https://doi.org/10.1002/anie.201903976>
9. Li G., Chu Y., Zhou Z. From AgGaS<sub>2</sub> to Li<sub>2</sub>ZnSiS<sub>4</sub>: Realizing impressive high laser damage threshold together with large second-harmonic generation response. *Journal Chemistry of Materials*. 2018;30(3): 602–606. DOI: <https://doi.org/10.1021/acs.chemmater.7b05350>
10. Yang J., Fan Q., Yu Y., Zhang W. Pressure effect of the vibrational and thermodynamic properties of chalcopyrite-type compound AgGaS<sub>2</sub>: A first-principles investigation. *Journal Materials*. 2018;11(12): 2370. DOI: <https://doi.org/10.3390/ma11122370>
11. Paderick S., Kessler M., Hurlburt T. J., Hughes S. M. Synthesis and characterization of AgGaS<sub>2</sub> nanoparticles: a study of growth and fluorescence. *Journal Chemical Communications*. 2018;54(1): 62–65. DOI: <https://doi.org/10.1039/C7CC08070K>
12. Kato K., Okamoto T., Grechin S., Umemura N. New Sellmeier and thermo-optic dispersion formulas for AgGaS<sub>2</sub>. *Journal Crystals*. 2019;9(3): 129–135. DOI: <https://doi.org/10.3390/cryst9030129>
13. Li W., Li Y., Xu Y., Lu J., Wang P., Du J., Leng Y. Measurements of nonlinear refraction in the mid-infrared materials ZnGeP<sub>2</sub> and AgGaS<sub>2</sub>. *Journal Applied Physics B*. 2017;123(3). DOI: 10.1007/s00340-017-6643-9
14. Jahangirova S. K., Mammadov Sh. H., Ajdarova D. S., Aliyev O. M., Gurbanov G. R. Investigation of the AgGaS<sub>2</sub>–PbS and some properties of phases of variable composition. *Russian Journal of Inorganic Chemistry*. 2019;64(9): 1169–1171. DOI: <https://doi.org/10.1134/S0036023619090092>
15. Asadov S. M., Mustafaeva S. N., Guseinov D. T. X-ray dosimetric characteristics of AgGaS<sub>2</sub> single crystals grown by chemical vapor transport. *Inorganic Materials*. 2017;53(5): 457–461. DOI: <https://doi.org/10.1134/S0020168517050028>
16. Mys O., Adamenko D., Skab I., Vlokh R. Anisotropy of acousto-optic figure of merit for the collinear diffraction of circularly polarized optical waves at the wavelength of isotropic point in AgGaS<sub>2</sub> crystals. *Ukrainian Journal of Physical Optics*. 2019;20(2): 73–80. DOI: <https://doi.org/10.3116/16091833/20/2/73/2019>
17. Karunagaran N., Ramasamy P. Investigation on synthesis, growth, structure and physical properties of AgGa<sub>0.5</sub>In<sub>0.5</sub>S<sub>2</sub> single crystals for Mid-IR application. *Journal of Crystal Growth*. 2018;483: 169–174. DOI: <https://doi.org/10.1016/j.jcrysgro.2017.11.030>
18. Ranmohotti K. G. S., Djieutedjeu H., Lopez J., Page A., Haldolaarachchige N., Chi H., Sahoo P., Uher C., Young D., Poudeu P. F. P. Coexistence of high-T<sub>c</sub> ferromagnetism and n-type electrical conductivity in FeBi<sub>2</sub>Se<sub>4</sub>. *J. of the American Chemical Society*. 2015;137(2): 691–698. DOI: <https://doi.org/10.1021/ja5084255>
19. Karthikeyan N., Aravindsamy G., Balamurugan P., Sivakumar K. Thermoelectric properties of layered type FeIn<sub>2</sub>Se<sub>4</sub> chalcogenide compound. *Materials Research Innovations*. 2018;22(5): 278–281. DOI: <https://doi.org/10.1080/14328917.2017.1314882>
20. Nakafsuji S., Tonomura H., Onuma K., Nambu Y., Sakai O., Maeno Y., Macaluso R. T., Chan J. Y. Spin disorder and order in quasi-2D triangular Heisenberg antiferromagnets: comparative study of FeGa<sub>2</sub>S<sub>4</sub>, Fe<sub>2</sub>Ga<sub>2</sub>S<sub>5</sub> and NiGa<sub>2</sub>S<sub>4</sub>. *Phys. Rev. Letters*. 2007;99(1–4): 157–203. DOI: <https://doi.org/10.1103/PhysRevLett.99.157203>
21. Rushchanskii K. Z., Haeuseler H., Bercha D. M. Band structure calculations on the layered compounds FeGa<sub>2</sub>S<sub>4</sub> and NiGa<sub>2</sub>S<sub>4</sub>. *J. Phys. Chem. Solids*. 2002;63(11): 2019–2028. DOI: [https://doi.org/10.1016/S0022-3697\(02\)00188-9](https://doi.org/10.1016/S0022-3697(02)00188-9)
22. Dalmas de Reotier P., Yaouanc A., MacLaughlin D. E., Songrui Zhao. Evidence for an exotic magnetic transition in the triangular spin system FeGa<sub>2</sub>S<sub>4</sub>. *J. Phys. Rev. B*. 2012;85(14): 140407.1–140407.5. DOI: <https://doi.org/10.1103/physrevb.85.140407>
23. Myoung B. R., Lim J. T., Kim C. S. Investigation of magnetic properties on spin-ordering effects of FeGa<sub>2</sub>S<sub>4</sub> and FeIn<sub>2</sub>S<sub>4</sub>. *Journal of Magnetism and Magnetic Materials*. 2017;438: 121–125. DOI: <https://doi.org/10.1016/j.jmmm.2017.04.056>
24. Asadov M. M., Mustafaeva S. N., Hasanova U. A., Mamedov F. M., Aliyev O. M., Yanushkevich K. I., Nikitov S. A., Kuli-Zade E. S. Thermodynamics of FeS–PbS–In<sub>2</sub>S<sub>3</sub> and properties of intermediate phases. *Journal Defect and Diffusion Forum*. 2018;385: 175–181. DOI: <https://doi.org/10.4028/www.scientific.net/DDF.385.175>
25. Li K., Yuan D., Shen S., Guo J. Crystal structures and property characterization of two magnetic frustration compounds. *Journal Powder Diffraction*. 2018;33(3): 190–194. DOI: <https://doi.org/10.1017/S0885715618000507>
26. Chen B., Zhu S., Zhao B., Lei Y., Wu X., Yuan Z., He Z. Differential thermal analysis and crystal growth of AgGaS<sub>2</sub>. *Journal of Crystal Growth*. 2008;310(3): 635–638. DOI: <https://doi.org/10.1016/j.jcrysgro.2007.10.067>
27. Sinyakova E. F., Kosyakov V. I., Kokh K. A. Oriented crystallization of AgGaS<sub>2</sub> from the melt system Ag–Ga–S. *J. Inorganic Materials*. 2009;45(11): 1217–1221. DOI: <https://doi.org/10.1134/S0020168509110041>
28. Chykhrij S. I., Parasyuk O. V., Halka V. O. Crystal structure of the new quaternary phase AgCd<sub>2</sub>GaS<sub>4</sub> and phase diagram of the quasibinary system AgGaS<sub>2</sub>–CdS. *Journal of Alloys and Compounds*. 2000;312(1–2): 189–195. DOI: [https://doi.org/10.1016/S0925-8388\(00\)01145-2](https://doi.org/10.1016/S0925-8388(00)01145-2)

29. Olekseyuk I. D., Parasyuk O. V., Halka V. O., Piskach L. V. F., Pankevych V. Z., Romanyuk Ya. E. Phase equilibria in the quasi-ternary system  $\text{Ag}_2\text{S}-\text{CdS}-\text{Ga}_2\text{S}_3$ . *J. Alloys and compounds*. 2001;325(10): 167–179. DOI: [https://doi.org/10.1016/S0925-8388\(01\)01361-5](https://doi.org/10.1016/S0925-8388(01)01361-5)
30. Brand G., Kramer V. Phase equilibrium in the quasi-binary system  $\text{Ag}_2\text{S}-\text{Ga}_2\text{S}_3$ . *Mater. Res. Bull.* 1976;11(11): 1381–1388. DOI: [https://doi.org/10.1016/0025-5408\(76\)90049-0](https://doi.org/10.1016/0025-5408(76)90049-0)
31. Lazarev V. B., Kish Z. Z., Peresh E. Yu., Semrad E. E. *Slozhnye khal'kogenidy v sisteme  $A^3-B^{333}-C^{VI}$*  [Complex chalcogenides in the  $A^3-B^{333}-C^{VI}$  system]. Moscow: Metallurgiya Publ; 1993. 229 p. (In Russ.)
32. Ugay Ya. A. *Vvedenie v khimiyu poluprovodnikov* [Introduction to the chemistry of semiconductors]. Moscow: Vysshaya shkola Publ.; 1975. 302 p. (In Russ.)
33. Pardo M. E., Dogguy-Smiri L., Flahaut J., Nguyen H. D. System  $\text{Ga}_2\text{S}_3-\text{FeS}$  Diagramme de phase – etude cristallographique. *Mater. Res. Bull.* 1981;16(11): 1375–1384. DOI: [https://doi.org/10.1016/0025-5408\(81\)90056-8](https://doi.org/10.1016/0025-5408(81)90056-8)
34. Wintenberger M. About the unit cells and crystal structures of  $\sim\text{M}\text{Ga}_2\text{X}_4$  ( $\text{M} = \text{Mn}, \text{Fe}, \text{Co}$ ;  $\text{X} = \text{S}, \text{Se}$ ) and  $\text{ZnAl}_2\text{S}_4$  Type. In: *Proc. VII Int. Conf. on Solid Compounds of Transition Elements, CNRS*. Grenoble, France: IA 14/1-3, 1983.
35. Rustamov P. G., Babaeva P. K., Azhdarova D. S., Askerova N. A., Ailazov M. R. Nature of interaction in  $\text{Mn}(\text{Fe}, \text{Co}, \text{Ni})-\text{Ga}(\text{In})-\text{S}(\text{Se})$  ternary systems. *Azerb. Khim. Zh.* 1984;15: 101–103.
36. Raghavan V.  $\text{Fe}-\text{Ga}-\text{S}$  (Iron-Gallium-Sulfur). *J. Phase Equil.* 1998;19: 267–268. DOI: <https://doi.org/10.1361/105497198770342319>
37. Ueno T., Scott S. D. Phase relations in the  $\text{Ga}-\text{Fe}-\text{S}$  system at 900 and 800 C. *The Canadian Mineralogist*. 2002;40(2): 568–570. DOI: <https://doi.org/10.2113/gscanmin.40.2.563>
38. Allazov M. R. The system of  $\text{FeS}-\text{GaS}-\text{S}$ . *Bulletin of Baku State University*. 2009;(2): 42–47. Available at: <http://static.bsu.az/w8/Xeberler%20Jurnali/Tebiet%202009%203/42-47.pdf>
39. Dogguy-Smiri L., Dung Nguyen Huy, Pardo M. P. Structure cristalline du polytype  $\text{FeGa}_2\text{S}_4 \alpha 1\text{T}$ . *Mater. Res. Bull.* 1980;15(7): 861–866. DOI: [https://doi.org/10.1016/0025-5408\(80\)90208-1](https://doi.org/10.1016/0025-5408(80)90208-1)
40. Hahn H., Klingler W. Unter such ungen uber ternare chalkogenide. I. Uber die, kristall structure iniger ternaerer sulfide, die sich vom  $\text{In}_2\text{S}_3$  ableiten. *Zeitschrift fur Anorganische und Allgemeine Chemie*. 1950;263(4): 177–190. DOI: <https://doi.org/10.1002/zaac.19502630406>
41. Dogguy-Smiri L., Pardo M. P. Etude cristallographique du systeme  $\text{FeS}-\text{Ga}_2\text{S}_3$ . *Compt. Rend. Acad. Sci.* 1978;287: 415–418.
42. Allazov M. R., Musaeva S. S., Abbasova R. F., Huseynova A. G. Phase crystallization regions along isothermal sections of  $\text{Fe}-\text{Ga}-\text{S}$  systems. *Bulletin of the Baku State University*. 2013; (3):11–14. Available at: <http://static.bsu.az/w8/Xeberler%20Jurnali/Tebiet%20202013%20203/11-15.pdf> (In Russ., abstract in Eng.)
43. Rzaguluev V. A., Kerimli O. Sh., Azhdarova D. S., Mammadov Sh. H., Aliev O. M. Phase equilibria in the  $\text{Ag}_8\text{SnS}_6-\text{Cu}_2\text{SnS}_3$  and  $\text{Ag}_2\text{SnS}_3-\text{Cu}_2\text{Sn}_4\text{S}_9$  systems. *Kondensirovannye sredyi mezhfaznye granitsy=Condensed Matter and Interphases*. 2019;21(4): 544–551. DOI: <https://doi.org/10.17308/kcmf.2019.21/2365> (In Russ., abstract in Eng.)

### Information about the authors

Sharafat H. Mammadov, PhD in Chemistry, Associate Professor, Senior Researcher, Institute of Catalysis and Inorganic Chemistry n.a. Academician M. F. Nagiyev of the Azerbaijan National Academy of Sciences, Baku, Azerbaijan; e-mail: [azxim@mail.ru](mailto:azxim@mail.ru). ORCID iD: <https://orcid.org/0000-0002-1624-7345>.

Author have read and approved the final manuscript.

Translated by Marina Strepetova  
Edited and proofread by Simon Cox